MULTIDISCIPLINARY OPTIMIZATION OF A SUPERSONIC TRANSPORT USING DESIGN OF EXPERIMENTS THEORY AND RESPONSE SURFACE MODELING

ANTHONY A. GIUNTA,* VLADIMIR BALABANOV,* DAN HAIM,†
BERNARD GROSSMAN,‡ WILLIAM H. MASON,§ LAYNE T. WATSON¶

Multidisciplinary Analysis and Design (MAD) Center for Advanced Vehicles
Virginia Polytechnic Institute and State University
Blacksburg, Virginia 24061-0203, U.S.A.
email: grossman@aoe.vt.edu

RAPHAEL T. HAFTKA#

Department of Aerospace Engineering, Mechanics and Engineering Science, University of Florida
Gainesville, Florida 32611-6250, U.S.A.
email: haftka@ufl.edu

ABSTRACT

The presence of numerical noise in engineering design optimization problems inhibits the use of many gradient-based optimization methods. This numerical noise may result in the inaccurate calculation of gradients which in turn slows or prevents convergence during optimization, or it may promote convergence to spurious local optima. The problems created by numerical noise are particularly acute in aircraft design applications where a single aerodynamic or structural analysis of a realistic aircraft configuration may require tens of CPU hours on a supercomputer. The computational expense of the analyses coupled with the convergence difficulties created by numerical noise are significant obstacles to performing aircraft multidisciplinary design optimization. To address these issues, a procedure has been developed to create noise-free algebraic models of subsonic and supersonic aerodynamic performance quantities for use in the optimization of high-speed civil transport (HSCT) aircraft configurations. This procedure employs methods from statistical design of experiments theory and response surface modeling to create the noise-free algebraic models. Results from a sample HSCT design problem involving ten variables are presented to demonstrate the utility of this method.

* Graduate Research Assistant, Dept. of Aerospace and Ocean Engineering
† Graduate Research Assistant, Dept. of Computer Science
‡ Professor and Head, Dept. of Aerospace and Ocean Engineering
§ Professor of Aerospace and Ocean Engineering
¶ Professor of Computer Science and Mathematics
# Professor of Aerospace Engineering, Mechanics and Engineering Science

NOMENCLATURE

ANOVA	analysis of variance
b_{half}	wing semi-span
$b_{nacelle}$	spanwise location of the inboard nacelle centerline
c	vector of unknown coefficients in least squares surface fitting
$\hat{c}$	vector of estimated coefficients in least squares surface fitting
C_D	drag coefficient
C_{Dlift}	supersonic drag-due-to-lift
C_{Dwave}	supersonic volumetric wave drag
C_l	wing section lift coefficient
C_L	lift coefficient
$C_{L\alpha}$	lift curve slope
C_{root}	root chord
C_{tip}	tip chord
C_T	leading edge thrust coefficient
CFD	computational fluid dynamics
CPU	central processing unit
DOE	design of experiments
g	vector of the optimization constraint values
HSCT	high-speed civil transport
k_t	attainable leading edge thrust factor
$(L/D)_{max}$	maximum value of the lift to drag ratio
LE	leading edge
M	Mach number
M_{fuel}	fuel mass
MDO	multidisciplinary design optimization
R^2	correlation coefficient in least squares surface fitting
$R^2{}_{adj}$	adjusted correlation coefficient
R_{LE}	leading edge radius parameter (dimensionless)
RMS	root mean square
RS	response surface
RSM	response surface methodology
SQP	sequential quadratic programming
t_{max}	chordwise location of maximum thickness (in percent chord)
t/c	thickness-to-chord ratio
TE	trailing edge
TOGM	takeoff gross mass
VCRSM	variable complexity response surface modeling
x	vector denoting a location in 10-dimensional space
$\mathbf{X}$	matrix of sample site locations in least squares surface fitting
Y	vector of observed response values at sample sites
Λ_{LE_I}	inboard leading edge sweep angle
Λ_{LE_O}	outboard leading edge sweep angle

1. INTRODUCTION

1.1 Motivation

Multidisciplinary design optimization (MDO) is the title given to a variety of methods by which several engineering disciplines are considered simultaneously in the design of a part or product. Thus, MDO is one implementation of concurrent engineering. The aircraft industry has given considerable attention to MDO as manufacturers attempt to reduce the time-to-market of new products. In traditional aircraft design, high fidelity analysis methods (e.g., Navier-Stokes fluid flow analyses and detailed finite element structural analyses) are not employed until late in the design process because of their computational expense. However, as the time-to-market of new products decreases, less time is available for the traditional aircraft design process. Therefore, aircraft MDO practitioners would like to use high fidelity analysis methods as early as possible in the design process where the increased accuracy of the high fidelity methods can most strongly influence aircraft design. However, the realities of finite computational resources and time constraints limit the extent to which the high fidelity analyses may be applied in the early stages of aircraft design.

One drawback to using high fidelity analyses is *numerical noise* which occurs as a result of the incomplete convergence of iterative processes, the use of adaptive numerical algorithms, round-off errors, and the discrete representation of continuous physical objects (fluids or solids). Such numerical noise is typically manifested as a high frequency, low amplitude variation in the results obtained from the computer analyses as the design parameters vary. When numerical optimization is attempted, this oscillatory behavior creates numerous, artificial local optima and causes slow convergence or even convergence failures[1,2]. Often the result is that the optimizer identifies many locally-optimal designs, each of which is obtained by starting the optimization process from a different initial design. Here, the optimization process is deterministic (i.e., the same optimal design is found for a specific set of initial variables), but the numerical noise traps the optimizer far from the globally-optimal design. The problems associated with numerical noise in optimization are ubiquitous in engineering, with examples appearing in structural optimization software[3,4], and in an Euler flow solver used for a supersonic nozzle design study[5].

Traditional, gradient-based optimization methods[6] and gradient-free pattern search methods[7] require *hundreds* or *thousands* of evaluations to converge to an optimal design for complex MDO problems. Thus, when a combined aerodynamic and structural analysis of an aircraft is computationally expensive, numerous local optima and convergence difficulties are unacceptable in aircraft MDO. While there are several computer programs which perform aircraft MDO using computationally inexpensive methods (e.g., ACSYNT[8], FLOPS[9]), high fidelity aircraft MDO in the presence of numerical noise remains computationally intractable. Clearly, new strategies are needed to alleviate the optimization problems posed by numerical noise, and this has spurred much current research in both the aircraft design and numerical optimization communities[10,11]. In one of these efforts, Gillmore and Kelley[12] have developed gradient-based optimization methods in which the finite difference step size is systematically varied until convergence is attained. This method has been successful on a number of problems in which numerical noise has posed optimization difficulties.

In efforts to develop a methodology that will be successful for aircraft MDO, Giunta[13] et al. proposed a method which is termed *variable complexity response surface modeling* (VCRSM). The unique aspect of this work stems from the use of a hierarchy of aerodynamic models (of increasing accuracy, complexity, and computational expense) during the aircraft design process. That is, the VCRSM method provides the aircraft designer with a strategy to identify promising aircraft configurations, based on some measure of merit, during each of the stages of the design process. It is this use of aerodynamic models of varying fidelity (i.e., variable complexity modeling) which distinguishes this work from that of others in the field of aircraft MDO (cf., Toomer[14] et al., and Chen[15] et al.).

In the aircraft MDO study presented here the multidisciplinary design optimization of a High-Speed Civil Transport (HSCT) aircraft (Figure 1) was used as a testbed for the VCRSM method. The design of an HSCT is an ideal MDO test case since the technical and economic feasibility of such an aircraft relies on synergistic interactions between the various aircraft design disciplines. Additional information is provided below on the specific application of the VCRSM method to the HSCT optimization problem.

1.2 Background

The *variable complexity* portion of VCRSM denotes the use of low, medium, and high fidelity aircraft analysis methods. Here the low fidelity methods include algebraic expressions for estimating lift and drag for HSCT-type aircraft. These typically require only a few CPU seconds to evaluate on a workstation. The medium fidelity methods include linear theory aerodynamic analyses These analyses require tens of CPU seconds up to several CPU minutes on a workstation. The high fidelity methods include various subsets of the Navier-Stokes equations including the Reynolds-averaged Navier-Stokes equations, the parabolized Navier-Stokes equations, and the Euler equations. These analyses require anywhere from tens of CPU minutes on a workstation to tens of CPU hours on a supercomputer. Thus, the computational expenses between a single low fidelity analysis and a single high fidelity analysis methods spans several orders of magnitude.

In optimization problems the *design space* refers to the box-like region of interest formed by the lower and upper bounds on each design variable. In VCRSM the low fidelity methods are used to perform aerodynamic analyses for *thousands* or *tens of thousands* of HSCT configurations in the design space. Such a large number of analyses is used to identify a subset of the design space where the HSCT configurations meet minimum values for several performance-related criteria. This portion of the design space is termed the *reasonable design space.* Next, *tens* to *hundreds* of HSCT configurations are selected from the reasonable design space and are evaluated using the medium and/or high fidelity analysis methods. In this manner, computational resources are not squandered in evaluating HSCT configurations outside of the reasonable design space which do not meet the minimum performance criteria.

The *response surface modeling* portion of VCRSM denotes the use of two statistical methods known as design of experiments theory[16] and response surface modeling[17]. Here, design of experiments (DOE) theory is used to systematically select the HSCT configurations which will be analyzed using the low fidelity analysis methods in the original design space and the medium/high fidelity analysis methods in the reasonable design space. Once the medium/high fidelity analyses are completed, response surface models (multidimensional curve fits) are created from the resulting aerodynamic data. Typically the response surface models are quadratic polynomials in the design variables although other curve fitting or interpolating models may be used. The response surface models are then employed as *approximation models* or *surrogate models* which replace the medium/high fidelity analysis methods when performing numerical optimization. The response surface models have two advantages over the medium/high fidelity analysis methods which are (1) the response surface models are computationally inexpensive to evaluate since they are algebraic equations, and (2) the response surface models remove the numerical noise present in the medium and high fidelity analysis results.

In many RSM applications quadratic polynomials are assumed to accurately model the selected response. Although this is certainly not true for all cases, RSM becomes prohibitively expensive when cubic and higher-order polynomials are chosen for experiments involving several variables. In addition, cubic and higher-order polynomials may yield surfaces that are not acceptable for numerical optimization. Giunta[1] et al. concluded that quadratic polynomial models were sufficiently accurate for HSCT configuration design.

In applying the VCRSM process the size of the design space has been reduced substantially. For example, in a two variable problem with the range of each variable reduced by one half, the reasonable design space contains one quarter of the area of the original design space. In a ten-variable problem, eliminating half of the range of each variable results in a reasonable design space with less than 0.10 percent of the volume of the original design space. The work of Kaufman[3] et al. and Roux[18] et al. showed that the response surface models were considerably more accurate when created for the reasonable design space than for the original design space.

Once the reasonable design space is identified and the response surface models are constructed, a traditional gradient-based numerical optimization is conducted for the aircraft MDO problem using the response surface models instead of the original computational methods. With the optimizer restricted to the reasonable design space and with the noise-free, computationally inexpensive response surface models, aircraft MDO is possible.

For this study a ten-variable HSCT design problem was selected to demonstrate the utility of the VCRSM method. Here the ten variables define the shape of the wing while the remaining portions of the HSCT (fuselage/tail/engine geometry) remain fixed. Response surface models were used as approximation models for four aerodynamic quantities as functions of the ten geometric variables which define the HSCT wing. These four aerodynamic quantities are supersonic volumetric wave drag, two components of supersonic drag-due-to-lift, and the subsonic lift curve slope.

High fidelity analysis tools are not included in this study because of their computational expense. However, the VCRSM method described here is easily extended to include data from high fidelity analyses. In this study the low fidelity analysis methods are used to identify the reasonable design space and medium fidelity analyses are used to construct the response surface models. An Euler/Navier-Stokes solver has been evaluated for use in HSCT design and these efforts are described in Reference 19. Although not discussed here, parallel computing is crucial in reducing the computational expense of using the VCRSM method for aircraft MDO. See Reference 20 for details on how parallel computing strategies are employed in the VCRSM method.

2. HSCT DESIGN OPTIMIZATION

2.1 Design Tools

The design problem is to minimize the takeoff gross mass (TOGM) for a 250 passenger High-Speed Civil Transport with a range of 10200 km and a cruise speed of Mach 2.4. The simplified mission profile includes takeoff, supersonic cruise, and landing. For these efforts we have developed a suite of low fidelity and medium fidelity analysis methods which include several software packages obtained from NASA along with in-house software. A description of these tools is given in Reference 2. The numerical optimization software is the commercially available program DOT[21] (Design Optimization Tools). DOT offers several algorithms for performing constrained optimization and its sequential quadratic programming (SQP) optimization option is employed in this study.

2.2 HSCT Wing Design Problem

A ten-variable HSCT wing design problem was examined to develop the VCRSM method. The ten variables for this design problem are wing root chord (C_{root}), wing tip chord (C_{tip}), wing semi-span (b_{half}), inboard leading edge sweep angle (Λ_{LE_I}), outboard leading edge sweep angle (Λ_{LE_O}), chordwise location of maximum thickness (t_{max}), leading edge radius parameter (R_{LE}), thickness-to-chord ratio (t/c), spanwise location of the inboard nacelle ($b_{nacelle}$), and fuel mass (M_{fuel}). Their initial values along with the minimum and maximum values are listed in Table 1. Figure 2 shows the airfoil and wing planform variables for this problem. For analysis purposes the HSCT wing is represented using 18 airfoil sections equally-spaced in the spanwise direction. In this wing definition C_{root} is the chord of the first airfoil section and C_{tip} is the chord of the eighteenth airfoil section.

For this optimization problem the area-ruled fuselage shape is held constant at a length of 91.4 m and an internal volume of 671.7 m^3. In addition, the vertical tail area is held constant at 65.0 m^2, and the thrust is fixed at a value of 175.2 kN per engine. Further, the outboard nacelle is held constant at a spanwise distance of 1.8 m from the centerline of the inboard nacelle and the Mach 2.4 cruise altitude is constant at 21300 m. To uniquely define the wing planform, the length of the leading edge from the wing/fuselage intersection to the leading edge break is fixed at a value of 45.7 m.

The 49 constraints for this optimization problem are listed in Table 2. The geometric constraints are applied to the HSCT configuration to prevent the optimizer from creating grossly unrealistic designs, such as wings with zero thickness or engine nacelles located inside the fuselage. These constraints are computationally inexpensive to evaluate since no aerodynamic or weight calculations are involved. Note that the 18 airfoil sections are constrained to have a minimum chord of 2.1 m. In addition, there is a constraint affecting the two most outboard airfoil sections (airfoil section spacing at wingtip ≥ 0.9 m) which prevents excessive aft sweep in the outboard wing sections which can be created for certain extreme values of the planform variables.

In contrast, the aerodynamic and performance constraints are considerably more computationally expensive than the geometric constraints. The range constraint is the most expensive of the aerodynamic constraints since the various supersonic aerodynamic analysis methods are used repeatedly in the range calculation (See Dudley[2] et al.). The least expensive of the aerodynamic constraints concern the section C_l and total C_L at landing. An elliptical spanwise lift distribution is assumed for the section C_l constraints, and lift equal to weight is assumed for the total C_L constraint. For both the section C_l and C_L constraints a worst-case emergency landing scenario is simulated with the following conditions (1) a landing velocity of 75 m/s (≈ 270 km/hr), (2) a landing mass which includes 50 percent of the total fuel mass, (3) an airport elevation of 1500 m above sea level, and (4) high temperatures ($32°C$) at the landing site.

Of moderate computational expense are the remaining performance constraints which encompass landing angle of attack limits and runway strike conditions. These landing-related constraints rely on the calculation of the subsonic lift curve slope. See Dudley[2] et al. for additional details on the calculation of these constraints.

With the ten variables and 49 constraints described above, the HSCT wing design optimization problem may be expressed as

$$\begin{aligned} &\min_{x \in R^{10}} TOGM(x) \\ &\text{subject to } g_i(x) \leq 0, \qquad i = 1, \ldots, 49. \end{aligned} \tag{1}$$

In this form x is the vector of ten design variables and g is the vector of 49 nonlinear inequality constraints.

3. NUMERICAL NOISE ISSUES

3.1 Noise Sources

The drag coefficient values predicted by some of the aerodynamic analysis methods are sensitive to slight changes in the shape of the aircraft wing. This sensitivity is illustrated in Figure 3 which shows supersonic volumetric wave drag (C_{Dwave}) calculated for an HSCT cruising at Mach 2.4. Here, C_{Dwave} is estimated using the Harris wave drag code[22] where all of the HSCT variables are held constant, with the exception of the wing semi-span which is varied from 15 to 30 m.

As the semi-span increases, numerical noise is created by a high frequency variation in the calculated wave drag values. Physically, wave drag should change smoothly as the wing shape is varied. Note that this numerical noise occurs on an extremely small scale with variations in wave drag on the order of 0.02 to 0.1 drag counts (one drag count corresponds to $C_D = 0.0001$). In the work of Knill[19] et al. the accuracy of the Harris wave drag code was estimated as 1-2 drag counts. Although the magnitude of the numerical noise in wave drag is below the accuracy of the Harris wave drag code, both TOGM and the mission range constraint are sensitive to variations in C_{Dwave} on the order of 0.1 drag counts. The sensitivity of the analysis models to values of C_{Dwave} is one quality which distinguishes optimization problems involving numerical noise from other optimization problems involving numerous local minima.

One method to counter the existence of numerical noise is to employ smoothing functions which capture the trends, if any, in a set of noisy data values. There are many numerical methods, both interpolating and non-interpolating, which may be used to perform the smoothing operation. One particularly attractive type of smoothing function is the polynomial model which has been employed extensively in the statistical community for modeling noisy data. Thus, the statistical literature contains numerous tools for creating polynomial models, as well as for estimating the accuracy of the models. Additional details on polynomial modeling methods are provided below.

In Figure 3 a quadratic polynomial is used as a smoothing function to model the noisy C_{Dwave} values. As is shown, the quadratic curve smoothes out the various scales of numerical noise present in the data while it preserves the overall trend in the variation in wave drag coefficient.

In addition to the C_{Dwave} analyses, two components of the supersonic drag-due-to-lift (C_{Dlift}) are affected by numerical noise as well. Here, supersonic drag-due-to-lift is calculated as

$$C_{Dlift} = \left(\frac{1}{C_{L\alpha}} - k_t \frac{C_T}{{C_L}^2}\right){C_L}^2, \tag{2}$$

where $C_{L\alpha}$ is the supersonic lift curve slope at $M = 2.4$, $C_T/{C_L}^2$ is the leading edge thrust term, and k_t is an attainable leading edge thrust factor. The numerical noise in the drag-due-to-lift evaluation occurs in the supersonic lift curve slope and leading edge thrust terms. The supersonic panel methods of Carlson[23] et al. utilize a wing discretization scheme that is sensitive to wing planform changes. Thus, slight modifications to the leading and trailing edge sweep angles, along with changes in the location where the Mach angle intersects the leading edge, produce noisy variations in the predicted drag. As was the case for the noise levels in the wave drag analyses, the numerical noise in the drag-due-to-lift calculations is within the intended accuracy of the analysis method.

3.2 Response Surface Models

The VCRSM method removes sources of numerical noise which adversely affect numerical optimization. This is accomplished by creating smooth, polynomial response surface models to replace the noise-producing aerodynamic analysis methods. Without numerical noise to inhibit optimization, there is a greater probability that the globally-optimal design will be found, regardless of the initial variable values used at the start of optimization. In this study, numerical noise created by the supersonic aerodynamic analysis methods is eliminated by using response surface models for C_{Dwave}, $C_T/{C_L}^2$, and $C_{L\alpha}$.

One of the most important advantages of using response surface models in optimization is that the computational expense of optimization is reasonable. This allows the design engineer to perform global optimization and reliability-based optimization, which are otherwise prohibitively computationally expensive. In addition, the use of response surface models allows the design engineer to quickly perform a variety of trade-off studies which provide information on the sensitivity of the optimal aircraft configuration to changes in performance criteria (constraints) and to off-design conditions.

The reduction in the computational expense of optimization when using response surface models motivates their use in the modeling of data obtained from expensive analysis methods, even though the expensive analysis methods may not produce numerical noise. One such relatively expensive analysis method is a vortex-lattice method (based on linear theory aerodynamics) which is used to estimate subsonic aerodynamic performance needed in the calculation of the HSCT landing constraints (See Table 2). In particular, the subsonic lift curve slope $C_{L\alpha}$ at $M = 0.2$ is needed in the calculation of these landing-related constraints. Thus, in addition to the three RS models noted above, a fourth RS model for $C_{L\alpha}$ at $M = 0.2$ is used in this investigation to reduce computational expense during optimization.

4. STATISTICAL METHODS

Experimental design theory[16] is a branch of statistics which provides the researcher with numerous methods for selecting the independent variable values at which a limited number of experiments will be conducted. The various experimental design methods create certain combinations of numerical experiments (analyses) in which the independent variables are prescribed at specific values or *levels.* The results of these planned experiments are used to investigate the sensitivity of some dependent quantity, identified as the *response,* to the independent variables. Other statistical techniques known as regression analysis and analysis of variance (ANOVA) are employed in the response sensitivity investigation. They are used to perform a systematic decomposition of the variability in the observed response values and to assign portions of the variability to either the effect of an independent variable or to experimental error. In using ANOVA with numerical experiments, numerical noise takes the place of experimental error.

4.1 Response Surface Modeling

A response surface methodology (RSM) is a modeling strategy combining elements of experimental design, regression analysis, and ANOVA[17]. RSM employs these statistical methods to create functions, typically linear or quadratic polynomials, to model the response or outcome of a numerical experiment in terms of several independent variables, e.g., wave drag expressed as a function of several wing planform variables.

A quadratic response surface (RS) model has the form

$$y = c_o + \sum_{1 \leq j \leq m} c_j x_j + \sum_{1 \leq j \leq k \leq m} c_{jk} x_j x_k \, , \tag{3}$$

where y is the response, x_j represents the m design variables, and c_o, c_j, and c_{jk} are the unknown polynomial coefficients. Note that there are $n = (m+1)(m+2)/2$ coefficients in this quadratic polynomial. To estimate the unknown polynomial coefficients in the RS model, at least p response values must be available, where $p \geq n$. Under such conditions, the estimation problem may be formulated in matrix notation as $Y \approx \mathbf{X}c$, where Y is the p by 1 vector of observed response values, $\mathbf{X}$ is a p by n matrix of constants assumed to have rank n, and c is the n by 1 vector of unknown coefficients to be estimated. The least squares solution to $Y \approx \mathbf{X}c$ is $\hat{c} = (\mathbf{X}^T\mathbf{X})^{-1}\mathbf{X}^T Y$. Typically, values for p of at least $1.5n$ to $2.5n$ are required to produce response surface models which accurately model the trends in the calculated data[1].

In addition to estimating the coefficients in the quadratic polynomial model, ANOVA and regression analysis also yield a measure of the uncertainty in the coefficients. This uncertainty estimation is provided by the t-statistic which is defined in Myers and Montgomery[17] as

$$t = \frac{c_{j-1}}{\sqrt{\hat{\sigma}^2 (\mathbf{X}^T\mathbf{X})^{-1}_{jj}}}, \tag{4}$$

where $\hat{\sigma}^2$ is the estimate of the variance in the observed response data and $j = 1, \ldots, n$. Note that the reciprocal of the t-statistic is an estimate of the standard deviation of each coefficient as a fraction of its value. Accordingly, coefficients with "low" values for the t-statistic are not accurately estimated. It is the prerogative of the user to select the minimum allowable t-statistic. This choice typically depends on the number of observed response values (also known as *degrees of freedom* (DOF) in the statistical lexicon) used to create the response surface model. For a coefficient estimated with at least of one degree of freedom, a 90 percent confidence interval requires a t-statistic of greater than 6.31 for that coefficient to be estimated accurately. This value of 6.31 is obtained from tabulated values of the probability density function of the t-distribution which are found in most text books on statistics (cf., Reference 24).

Various procedures exist for removing terms in a polynomial model which are not accurately estimated (i.e., terms for which the coefficients have a low t-statistic). Allowing these poorly estimated terms to remain in the response surface polynomial model may actually reduce the prediction accuracy of the model. A common statistical measure of the utility of removing terms from a polynomial model is the adjusted R^2 value (${R^2}_{adj}$). The adjusted R^2 value is calculated as

$${R^2}_{adj} = 1 - \frac{SSE/DOF_{SSE}}{SYY/DOF_{SYY}}, \tag{5}$$

where SSE is the error sum of squares, SYY is the total sum of squares, and the DOF for SSE and SYY are obtained from ANOVA calculations[17]. The maximum value for ${R^2}_{adj}$ is 1.0 which occurs when all of the variation in the observed response values is described by the trends of the response surface polynomial model. Typical values for ${R^2}_{adj}$ range from 0.9 to 1.0 when the observed response values are accurately predicted by the response surface model.

For this study the commercial statistical package JMP[25] was used to perform ANOVA and regression analysis along with other statistical analyses. See the JMP User's Manual and the text by Myers and Montgomery for a description of the statistical methods which underlie ANOVA and regression analysis, including the calculation of R^2 and $R^2{}_{adj}$.

4.2 Experimental Design Methods

4.2.1 Full Factorial Experimental Designs

Prior to creating an experimental design, the allowable range of each of the m variables is defined by lower and upper bounds. The allowable range is then discretized at equally-spaced levels. For numerical stability and for ease of notation, Myers and Montgomery[17] suggest that each variable should be scaled to the interval $[-1, 1]$. The region enclosed by the lower and upper bounds on the variables is termed the design space, the vertices of which determine an $m-$dimensional cube. If each of the variables is specified at only the lower and upper bounds (two levels), the experimental design is called a 2^m full factorial. Similarly, a 3^m full factorial design is created by specifying the lower bound, midpoint, and upper bound (three levels) for each of the m variables. A 3^3 full factorial design is shown in Figure 4.

The construction of a quadratic response surface model in m variables requires at least $n = (m+1)(m+2)/2$ response evaluations. A 3^m full factorial design provides ample response evaluations to permit the estimation of the RS model coefficients. For example, fitting a quadratic response surface model in three variables ($m = 3$) requires at least ten evaluations, and a 3^3 full factorial design provides 27 evaluations. However, as m becomes large the evaluation of both 2^m and 3^m full factorial designs becomes impractical (e.g., $2^{30} \approx 1.1 \cdot 10^9$). A full factorial design typically is used for ten or fewer variables. For greater than ten variables, an experimental design known as a partially balanced incomplete block (PBIB) design may be applied. See Kaufman[3] et al. for more details on PBIB experimental designs.

4.2.2 D-Optimal Experimental Designs

RSM typically employs a full factorial or similar experimental design. However, full factorial designs are intended for use with rectangular design spaces and not the irregularly shaped (even nonconvex) design spaces that may arise in the HSCT design problems considered here. Previous studies[1,26,27] found that the D-optimality criterion[28] provides a rational means for creating experimental designs inside an irregularly shaped design space.

The objective of the D-optimality criterion is to select the set of p locations in a design space from a pool of q candidate locations ($q \geq p$), such that the quantity $|\mathbf{X}^T\mathbf{X}|$ is maximized. Note that the pool of q candidate locations is defined *a priori* by the user, and the p locations which maximize $|\mathbf{X}^T\mathbf{X}|$ are found iteratively using a numerical optimization method. The set of p locations for which $|\mathbf{X}^T\mathbf{X}|$ is maximum is called a D-optimal experimental design. The statistical reasoning behind the creation of a D-optimal design is that it leads to response surface models for which the uncertainty in the estimated coefficients is minimized.

For this study, a computer program employing the "k-exchange" method of Mitchell[29] was used to select a set of p D-optimal locations from a user supplied list of q candidate locations. In addition, the commercial statistical package JMP[25] was used to perform ANOVA calculations. Earlier work[1,3,20,27] used genetic algorithms to create D-optimal experimental designs.

5. THE VCRSM METHOD

The construction of the response surface models may be viewed as a series of steps to be completed before the HSCT optimization is performed. This methodology is illustrated in the flowchart shown in Figure 5. Starting from an initial HSCT configuration, a 3^m or similar full factorial design is constructed with the initial HSCT at the center of the design space. The HSCT configurations selected in the full factorial design are evaluated using the computationally inexpensive low fidelity analysis tools. The analysis results for the HSCT configurations are then screened to eliminate any grossly infeasible HSCT configurations, where an HSCT configuration was eliminated if it violated any of the geometric, section C_l, or C_L constraints by more than five percent. The HSCT configurations which remain comprise the reasonable design space. Next, the D-optimality criterion is applied to select a subset of the HSCT configurations in the reasonable design space for evaluation using the medium fidelity analysis methods. Response surface models for the aerodynamic quantities are then constructed using the medium fidelity analysis data. In the final step of the VCRSM method the response surface models are used in the HSCT optimization software to replace the noise-producing aerodynamic analysis methods. Then a gradient-based optimization is performed without the convergence problems caused by numerical noise.

6. HSCT DESIGN PROBLEM

6.1 Low Fidelity HSCT Analyses

A 3^{10} full factorial design (i.e., three levels in each variable) was constructed around an initial HSCT configuration. The 59049 (3^{10}) full factorial design points were analyzed using the inexpensive, low fidelity analysis tools and the HSCT analysis results were screened to eliminate from consideration any grossly infeasible HSCT configurations. After screening, 29163 HSCT configurations remained in the reasonable design space; 51 percent of the original HSCT candidate configurations were eliminated.

6.2 Medium Fidelity HSCT Analyses

The next step in the VCRSM process was to select a set of 132 D-optimal HSCT configurations from the remaining candidate set of 29163. For this problem, an in-house version of Mitchell's k-exchange algorithm was used to create the D-optimal experimental design. The distribution of the 132 D-optimal HSCT configurations within the design space gives a condition number of 27 for the matrix $\mathbf{X}$. This indicates that $\mathbf{X}$ has full rank and that $(\mathbf{X}^T\mathbf{X})^{-1}$ exists.

The 132 D-optimal HSCT configurations were evaluated using the medium fidelity analysis methods. Quadratic RS models, each having 66 coefficients, were created for C_{Dwave}, $C_{L\alpha}$ at $M = 2.4$, $C_T/{C_L}^2$, and $C_{L\alpha}$ at $M = 0.2$. The ${R^2}_{adj}$ values for these RS models were 0.9603, 0.9976, 0.9982, and 0.9979, respectively. Regression analyses were performed on these RS models and coefficients that did not have a t-statistic greater than 6.31 were removed. The recomputed ${R^2}_{adj}$ values for the RS models were 0.9667, 0.9978, 0.9986, and 0.9983, respectively.

The results of the regression analyses are shown in Table 3 where the important linear and quadratic terms in the four RS models are listed. The RS model for C_{Dwave} was most strongly influenced by 17 coefficients which included all of the linear terms except for $C_{tip}, b_{nacelle}$, and M_{fuel}, and included the quadratic terms for t/c and Λ_{LE_I}. The RS model for $C_{L\alpha}$ ($M = 2.4$) was comprised of 31 coefficients which included all of the linear terms except for t_{max}, and included the quadratic terms for $C_{root}, b_{half}, R_{LE}, t/c$, and Λ_{LE_I}. The RS model for $C_T/{C_L}^2$ employed 17 coefficients which contained the linear terms for $C_{root}, C_{tip}, b_{half}$, R_{LE}, Λ_{LE_I}, and Λ_{LE_O}, along with the quadratic terms for C_{root}, Λ_{LE_I}, and Λ_{LE_O}. The RS model for $C_{L\alpha}$ ($M = 0.2$) was populated with 18 coefficients which included the linear terms for $C_{root}, C_{tip}, b_{half}, t/c, \Lambda_{LE_I}$, and Λ_{LE_O}, along with the quadratic terms for C_{root}, b_{half}, and Λ_{LE_I}. In summary, all of the linear coefficients were important in at least one of the RS models and six of the quadratic coefficients ($C_{root}, t/c, b_{half}$, R_{LE}, Λ_{LE_I}, Λ_{LE_O}) were important in at least one of the RS models.

Another quantitative measure of the quality of the RS model is to evaluate the residual error in the least squares fit which creates the RS model. The residual error is the difference between the calculated response from the numerical experiment data and the predicted response from the RS model. The residual error is a composite measure of error due to numerical noise and error due to bias. Bias error occurs when using a low order polynomial RS model for data with higher order trends. The average error, RMS error, and maximum error for the complete RS models (66 coefficients) are shown in Table 4, where the residual error calculations are performed for the data from the 132 HSCT analyses used to create the RS models.

For C_{Dwave} the residual error is the result of bias error since the magnitude of the numerical noise in the C_{Dwave} data is known to be small compared to typical values of C_{Dwave} (see Section 3.1). In contrast, for $C_T/{C_L}^2$ the residual error is mostly due to numerical noise. It is known that the leading edge thrust estimation methods are extremely sensitive to changes in the HSCT wing planform. This sensitivity produces numerical noise in the $C_T/{C_L}^2$ data where the magnitude of the noise may be up to 25 percent of typical $C_T/{C_L}^2$ values[30]. Although a predicted value for $C_T/{C_L}^2$ from the RS model may contain significant error, the supersonic drag-due-to-lift calculation is dominated by the $C_{L\alpha}$ ($M = 2.4$) term. Thus, there is minimal effect on the overall HSCT wing design due to the residual error in the $C_T/{C_L}^2$ RS model. Also, note that for the initial HSCT configuration the range computed using the RS models is 10200 km and the range computed using the original methods is 10230 km, a difference of 0.29 percent.

6.3 HSCT Optimization with Response Surface Models

Using the RS models, the HSCT configuration was optimized within the allowable limits of the ten variables. To verify that the numerical noise was removed from the optimization problem by using the RS models, two optimization cases were performed where each case started from a distinctly different initial HSCT configuration. For the first of these cases, Figure 6 shows the wing planform changes from the initial to the optimal HSCT configuration and the initial and optimal variables are listed in Table 5. The optimal HSCT has a smaller wing area and a lower aspect ratio than the initial HSCT which results in a wing structural mass savings of about 10660 kg, a decrease of approximately 18 percent. In addition to the structural improvements, the $(L/D)_{max}$ of the HSCT increased from 9.37 to 9.54, an improvement of 1.8 percent. This contributes to a savings in fuel mass of approximately 8160 kg. The wings for the initial and optimal HSCT configurations are also shown in an isometric view in Figure 7 where the difference in the chordwise location of maximum thickness is more apparent. Similar mass savings were realized for the second optimization case where the optimizer converged to an HSCT design having a wing configuration virtually identical to the optimal HSCT design found in the first optimization case. Henceforth, this optimal HSCT configurations is denoted as the *RS optimal HSCT configuration*.

6.4 HSCT Optimization without Response Surface Models

When the two optimization cases were attempted without using the RS models (i.e., using the original numerical noise-producing aerodynamic modeling methods) the two HSCT configurations converged to substantially different locally-optimal HSCT configurations. One such locally-optimal design is shown in Figure 8. Also, note that both of these locally-optimal HSCT configurations had a higher value for TOGM than did the RS optimal HSCT configuration. This is consistent with the occurrence of multiple local optima and the convergence difficulties which originally motivated the use of RS modeling methods. The locally-optimal HSCT configuration in Figure 8 is about 7700 kg heavier than the RS optimal HSCT configuration. The optimization results, both with and without using the RS models, are shown in Table 6 for the two HSCT optimization cases.

6.5 Post Optimization Investigation

The RS optimal HSCT configuration has a mission range of 10200 km when the RS models are used to calculate supersonic drag. However, if the RS optimal HSCT configuration is evaluated using the original, and more accurate, aerodynamic models, the mission range is 10000 km. This 200 km discrepancy is the result of modeling error in the RS polynomials, which results in an underestimation of the total drag on the HSCT. Since the true range is below 10200 km, the HSCT configuration would need to carry additional fuel to meet the range requirement. This would add approximately 4200 kg to the TOGM of the RS optimal HSCT configuration which is an increase of 1.57 percent.

To further analyze the RS optimal HSCT configuration an additional optimization was performed to determine if the RS optimal HSCT was also optimal (or at least nearly optimal) when the original aerodynamic analysis models were employed. This optimization case used the RS optimal HSCT configuration listed in Table 5 for the ten initial variables and the upper and lower bounds listed in Table 1 for the side constraints.

The new optimal HSCT configuration found from this optimization case was nearly identical to the RS optimal HSCT configuration. The only variable which changed substantially was the fuel mass which increased by about 4250 kg to meet the mission range constraint of 10200 km. Note that even with the added fuel mass, the new optimal HSCT configuration has a lower TOGM than either of the two locally-optimal HSCT configurations listed in Table 6.

Numerical noise in the original aerodynamic models prevents the aircraft designer from knowing whether or not the globally-optimal HSCT configuration has been found. In the VCRSM method the designer avoids locally-optimal HSCT configurations created by numerical noise, and is more likely to identify the region of the design space in which the globally-optimal HSCT configuration exists.

6.6 Computational Expense

The computational expense of performing a complete ten-variable HSCT optimization using the RS models is approximately 1.5 CPU minutes on a Silicon Graphics Indigo^2 workstation. In comparison, an optimization without using the RS models requires about one CPU hour. Thus, the computational expense of performing an HSCT optimization was significantly reduced. However, this comparison does not include the computational overhead involved in creating the RS models.

The aggregate computational cost of creating the RS models is about 55 CPU hours when the HSCT analyses are performed serially. This includes approximately 50 CPU hours for the 3^{10} low fidelity analyses which require 2-3 CPU seconds per analysis, and five CPU hours for the 132 D-optimal medium fidelity analyses which require 1.5-2 CPU minutes per analysis. The majority of the computational expense occurs in the brute force approach of screening the initial design space on the 3^{10} grid. Clearly this approach will be far too computationally expensive in higher dimensional problems. In future research efforts we may perform this screening using a partially balanced incomplete block design as was done by Kaufman[3] et al. or we may model the initial design space using cubic polynomials. Either approach requires far fewer than the 3^{10} analyses performed in this study.

Although the overhead cost of the VCRSM method appears substantial, this cost is recovered when one considers that optimizations without the RS models must be repeated numerous times, each with different initial values for the variables, until the general region of the optimal HSCT configuration is located. Further, in aircraft design engineering, an aircraft configuration is almost never declared "optimal" without performing considerable trade-off studies. If the aircraft design is re-optimized during the trade-off studies, then the computational expense is virtually nil when the RS models are used. However, each re-optimization in the trade-off study requires about one CPU hour if RS models are not used.

6.7 VCRSM Versus Traditional Response Surface Modeling

If a traditional DOE and RS modeling approach had been followed in this investigation, RS models would have been calculated for the entire original design space rather than for only the reasonable design space. For this application, the reasonable design space has about 50 percent of the volume of the original design space. Thus, one would expect the RS approximations for the reasonable design space to be more accurate than RS approximations for the entire design space.

To investigate this question of RS model accuracy, 132 HSCT configurations were selected based on the D-optimal criterion from the set of 3^{10} HSCT configurations defined by the full-factorial experimental design in the original design space. These 132 HSCT configurations were evaluated using the medium fidelity analysis methods and response surface models were constructed for the four aerodynamic quantities previously described. These RS models are valid over the entire original design space.

Next, 150 HSCT configurations were randomly selected from the 29163 HSCT configurations in the reasonable design space and were evaluated using the medium fidelity analyses. From this *exact* data for the randomly selected HSCT configurations, the average, RMS, and maximum errors were calculated for each of the four aerodynamic quantities using the RS models obtained for the original design space and for the reasonable design space (Table 7).

As shown in Table 7, the RS models for the reasonable design space are more accurate than the RS models for the original design space for $C_T/{C_L}^2, C_{L\alpha}$ at $M = 2.4$, and $C_{L\alpha}$ at $M = 0.2$. Somewhat surprisingly, the error calculations indicate that accuracy of the RS model for C_{Dwave} is slightly lower for the reasonable design space as compared to the original design space. Further investigations showed that errors in the RS model for C_{Dwave} were particularly sensitive to the location in the design space of the 150 randomly selected points. Thus, the errors calculated for C_{Dwave} using both sets of RS models are not significantly different. Although the improvements in accuracy shown here for three of the four RS models are not quite as substantial as those shown by Kaufman[3] et al., this investigation demonstrates that a significant improvement in accuracy is obtained by limiting the response surface construction to the reasonable design space.

7. CONCLUSIONS

Design of experiments theory and response surface modeling methods have been combined to create *variable complexity response surface modeling,* a novel approach to optimization. The variable-complexity portion of VCRSM employs low fidelity analysis methods to eliminate portions of the original design space where the constraints on the optimization problem are grossly violated. Then, the remaining portions of the design space, termed the *reasonable design space*, are investigated using medium and/or high fidelity analysis methods. Design of experiments theory and response surface modeling are applied to construct polynomial response surface models for several aerodynamic quantities which are only valid in the reasonable design space. The original aerodynamic quantities are computationally expensive to evaluate and produce numerical noise; two qualities that inhibit the application of gradient-based optimization methods to engineering problems. The computationally inexpensive and noise-free response surface models are then used during optimization in lieu of the original analysis methods. An additional benefit of the computationally inexpensive response surface models is that they facilitate global and reliability-based optimization studies as well as the numerous trade-off studies often conducted in aircraft design engineering.

In this study, the VCRSM method is demonstrated on a multidisciplinary design optimization problem involving a high-speed civil transport aircraft subject to realistic aerodynamic and performance constraints. The HSCT optimization is formulated as a nonlinear programming problem involving ten variables and 49 constraints, with the objective of minimizing the takeoff gross mass of the aircraft. When the VCRSM method is applied to this problem, a potential globally-optimal HSCT configuration is identified. In contrast, without using the VCRSM method only inferior locally-optimal HSCT configurations are found. For the HSCT configurations examined in this study, typical savings in TOGM of 3500 to 7700 kg were obtained for aircraft having a total mass of approximately 277500 kg. This corresponds to a savings in TOGM of 1.3 to 2.7 percent.

ACKNOWLEDGEMENTS

This research was supported by NASA Grant NAG-1-1562.

REFERENCES

1. Giunta, A. A., Dudley, J. M., Narducci, R., Grossman, B., Haftka, R. T., Mason, W. H., and Watson, L. T. Noisy aerodynamic response and smooth approximations in HSCT design, Proceedings of the 5th AIAA/USAF/NASA/ISSMO Symposium on Multidisciplinary Analysis and Optimization, Panama City Beach, FL, 1994, pp. 1117–1128.
2. Dudley, J., Huang, X., MacMillin, P. E., Grossman, B., Haftka, R. T., and Mason, W. H. Multidisciplinary optimization of the High-Speed Civil Transport, AIAA Paper 95–0124, 1995.
3. Kaufman, M., Balabanov, V., Burgee, S., Giunta, A. A., Grossman, B., Mason, W. H., Watson, L. T., and Haftka, R. T. Variable-complexity response surface approximations for wing structural weight in HSCT design, AIAA Paper 96-0089, 1996.
4. Venter, G., Haftka, R. T., and Starnes, J. H., Jr. Construction of Response Surfaces for Design Optimization Applications, Proceedings of the 6th AIAA/USAF/NASA/ISSMO Symposium on Multidisciplinary Analysis and Optimization, Bellevue, WA, 1996, pp. 548–564.
5. Narducci, R., Grossman, B., Valorani, M., Dadone, A., and Haftka, R. T. Optimization methods for non-smooth or noisy objective functions in fluid design problems, Proceedings of the AIAA 12th Computational Fluid Dynamics Conference, San Diego, CA, 1995, pp. 21–32.
6. Gill, P. E., Murray, W., and Wright, M. H. Practical Optimization, Academic Press, Inc., San Diego, CA, 1981.
7. Nelder, J. A., and Mead, R. A Simplex Method for Function Minimization, Comput. J., 1965, 7, pp. 308–313.
8. Jayaram, S., Myklebust, A., and Gelhausen, P. ACSYNT – a standards-based system for parametric computer aided conceptual design of aircraft, AIAA Paper 92–1268, 1992.

9. McCullers, L. A. Aircraft configuration optimization including optimized flight profiles, Proceedings of the Symposium on Recent Experiences in Multidisciplinary Analysis and Optimization, J. Sobieski (ed.), NASA CP-2327, 1984, pp. 396–412.
10. Frank, P. D., Booker, A. J., Caudell, T. P., and Healy, M. J. A comparison of optimization and search methods for multidisciplinary design, Proceedings of the 4th AIAA/USAF/NASA/OAI Symposium on Multidisciplinary Analysis and Optimization, Cleveland, OH, 1992, pp. 1040–1057.
11. Sobieszczanski-Sobieski, J., Haftka, R. T. Multidisciplinary aerospace design optimization: survey of recent developments, AIAA Paper 96–0711, 1996.
12. Gilmore, P., and Kelley, C. T., An implicit filtering algorithm for optimization of functions with many local minima, SIAM J. Opt., 1995, 5, (2), pp. 269–285.
13. Giunta, A. A., Balabanov, V., Haim, D., Grossman, B., Mason, W. H., Watson, L. T., and Haftka, R. T. Wing design for a High-Speed Civil Transport using a design of experiments methodology, Proceedings of the 6th AIAA/NASA/ISSMO Symposium on Multidisciplinary Analysis and Optimization, Bellevue, WA, 1996, pp. 168–183.
14. Toomer, C. A., Topliss, M. E., and Hills, D. P. Aerodynamic optimisation using analytic descriptions of the design space, AIAA Paper 96–4141, 1996.
15. Chen, W., Allen, J. K., Schrage, D. P., and Mistree, F. Statistical experimentation methods for achieving affordable concurrent systems design, AIAA. J., 1997, 35, (5), pp. 893–900.
16. Montgomery, D. C. Design and Analysis of Experiments, John Wiley & Sons, New York, NY, 1976.
17. Myers, R. H., and Montgomery, D. C. Response Surface Methodology: Process and Product Optimization Using Designed Experiments, John Wiley & Sons, New York, NY, 1995.
18. Roux, W. J., Stander, N., and Haftka, R. T., Response surface approximations for structural optimization, Proceedings of the 6th AIAA/NASA/ISSMO Symposium on Multidisciplinary Analysis and Optimization, Bellevue, WA, 1996, pp. 565–578.
19. Knill, D. L., Balabanov, V., Grossman, B., Mason, W. H., and Haftka, R. T. Certification of a CFD code for High-Speed Civil Transport design optimization, AIAA Paper 96–0330, 1996.
20. Burgee, S., Giunta, A. A., Balabanov, V., Grossman, B., Mason, W. H., Narducci, R., Haftka, R. T., and Watson, L. T. A coarse grained parallel variable-complexity multidisciplinary optimization paradigm, Intl. J. Supercomputing Applications and High Performance Computing, 1996, 10, (4), pp. 269-299.
21. DOT Users Manual Version 4.20, Vanderplaats Research & Development, Inc., Colorado Springs, CO, 1995.
22. Harris, R. V., Jr. An analysis and correlation of aircraft wave drag, NASA TM X-947, 1964.
23. Carlson, H. W., and Walkley, K. B., Numerical methods and a computer program for subsonic and supersonic design and analysis of wings with attainable thrust considerations, NASA CP 3808, 1984.
24. Hogg, R. V., and Ledolter, J., Applied Statistics for Engineers and Physical Scientists, Macmillin, New York, NY, 1992.
25. JMP Users Guide Version 3.1, SAS Institute, Inc., Cary, NC, 1995.
26. Craig, J. A., Jr. D-optimal design method: final report and user's manual, General Dynamics Report FZM-6777 for Air Force Contract F33615-78-C-3011, 1978.
27. Giunta, A. A., Narducci, R., Burgee, S., Grossman, B., Mason, W. H., Watson, L. T., and Haftka, R. T. Variable-complexity response surface aerodynamic design of an HSCT wing, Proceedings of the 13th AIAA Applied Aerodynamics Conference, San Diego, CA, 1995, pp. 994–1002.
28. Box, M. J., and Draper, N. R. Factorial designs, the $|\mathbf{X}^T\mathbf{X}|$ criterion, and some related matters, Technometrics, 1971, 13, (4), pp. 731–742.
29. Mitchell, T. J. An algorithm for the construction of D-optimal experimental designs, Technometrics, 1974, 16, (2), pp. 203-210.
30. Hutchison, M. G. Multidisciplinary Optimization of High-Speed Civil Transport Configurations Using Variable-Complexity Modeling, Ph.D. Dissertation, Virginia Polytechnic Institute and State University, 1993.

Table 1. Nominal values for the ten HSCT wing variables and the allowable range on each variable.

Variable	Nominal	Min.	Max.
C_{root}	53.0 m	42.4 m	63.6 m
C_{tip}	2.5 m	2.0 m	3.0 m
b_{half}	22.5 m	20.3 m	24.8 m
Λ_{LE_I}	71.9°	65.4°	78.3°
Λ_{LE_O}	44.2°	40.2°	48.2°
t_{max}	39.6%	31.7%	47.5%
R_{LE}	2.6	2.1	3.2
t/c	2.3%	1.8%	2.7%
$b_{nacelle}$	6.4 m	5.1 m	7.7 m
M_{fuel}	140570 kg	136350 kg	144780 kg
$TOGM$	284170* kg	276770* kg	297950* kg

* Violates constraints.

Table 2. Constraints for the ten-variable HSCT optimization problem.

Num.	Geometric Constraints
1	Fuel volume $\leq$ 50% wing volume
2	Airfoil section spacing at wingtip ≥ 0.9 m
3-20	Wing chord ≥ 2.1 m
21	Leading edge break $\leq$ semi-span
22	Airfoil $t/c \geq 1.5\%$
Num.	**Aero. & Performance Constraints**
23	Range ≥ 10200 km
24	C_L at landing ≤ 1.0
25-42	Section C_l at landing ≤ 2.0
43	Landing angle of attack $\leq 13°$
44-45	Engine clearance ≥ 0.0 m, landing at 0° roll
46-47	Engine clearance ≥ 0.0 m, landing at 5° roll
48-49	Wing clearance ≥ 0.0 m, landing at 5° roll

Table 3. Important linear and
quadratic terms in the response surface models
(interaction terms not shown).

	$\mathbf{C_{Dwave}}$	$\mathbf{C_{L\alpha}}$ **(M=2.4)**	$\mathbf{C_T/C_L{}^2}$	$\mathbf{C_{L\alpha}}$ **(M=0.2)**
Linear Terms				
C_{root}	X	X	X	X
C_{tip}		X	X	X
b_{half}	X	X	X	X
Λ_{LE_I}	X	X	X	X
Λ_{LE_O}	X	X	X	X
t_{max}	X			
R_{LE}	X	X	X	
t/c	X	X		X
$b_{nacelle}$		X		
M_{fuel}		X		
Quadratic Terms				
C_{root}^2		X	X	X
C_{tip}^2				
b_{half}^2		X		X
$\Lambda_{LE_I}^2$	X	X	X	X
$\Lambda_{LE_O}^2$			X	
t_{max}^2				
R_{LE}^2		X		
$(t/c)^2$	X	X		
$b_{nacelle}^2$				
M_{fuel}^2				

Table 4. Accuracy of the responses
in the reasonable design space based on analyses
of the 132 D-optimal HSCT configurations.

	Avg. Error	**RMS Error**	**Max. Error**
C_{Dwave}	4.36%	5.78%	18.31%
$C_{L\alpha}$ at $M = 2.4$	0.21%	0.27%	0.91%
$C_T/C_L{}^2$	8.39%	13.19%	47.45%
$C_{L\alpha}$ at $M = 0.2$	0.24%	0.30%	0.90%

Table 5. HSCT optimization problem initial and optimal values for the ten variables.

Variable	Initial	Optimal
C_{root}	45.7 m	51.1 m
C_{tip}	2.7 m	2.5 m
b_{half}	24.4 m	22.4 m
Λ_{LE_I}	68.0°	71.1°
Λ_{LE_O}	47.0°	40.3°
t_{max}	33.0 %	47.5 %
R_{LE}	2.5	2.1
t/c	2.1 %	2.3 %
$b_{nacelle}$	5.5 m	5.1 m
M_{fuel}	144650 kg	136350 kg
$TOGM$	297320* kg	277540 kg

* Violates constraints.

Table 6. Optimization results for the two initial HSCT configurations, both with and with the response surface models.

	TOGM
Initial HSCT #1 *	297320 kg
Optimal HSCT [a]	277540 kg
Optimal HSCT [b]	285370 kg
Initial HSCT #2 *	284170 kg
Optimal HSCT [a]	277590 kg
Optimal HSCT [b]	283950 kg

[a] Optimization with response surface models.
[b] Optimization without response surface models.

* Violates constraints.

Table 7. Response surface modeling error estimates based on analyses of 150 randomly selected HSCT configurations.

	Avg. Error	RMS Error	Max. Error
(a) C_{Dwave}	6.89%	8.33%	30.85%
(b) C_{Dwave}	7.10%	9.40%	40.91%
(a) $C_{L\alpha}$ at $M = 2.4$	0.66%	0.82%	2.18%
(b) $C_{L\alpha}$ at $M = 2.4$	0.40%	0.58%	1.82%
(a) $C_T/{C_L}^2$	28.70%	47.28%	157.57%
(b) $C_T/{C_L}^2$	12.03%	18.93%	73.59%
(a) $C_{L\alpha}$ at $M = 0.2$	1.42%	1.81%	4.59%
(b) $C_{L\alpha}$ at $M = 0.2$	0.45%	0.56%	1.49%

[a] Response surface model – original design space.
[b] Response surface model – reasonable design space.

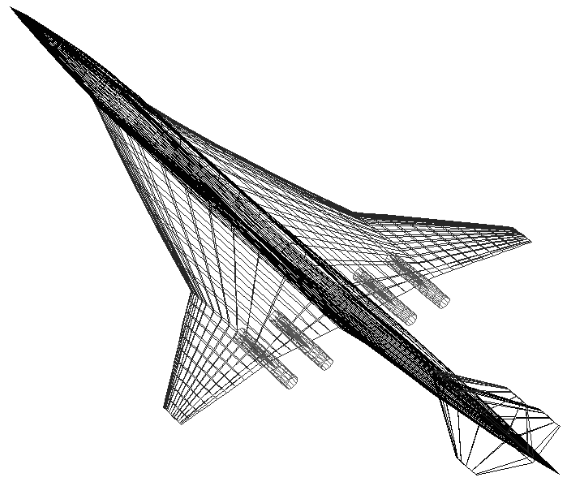

Figure 1. A typical HSCT configuration.

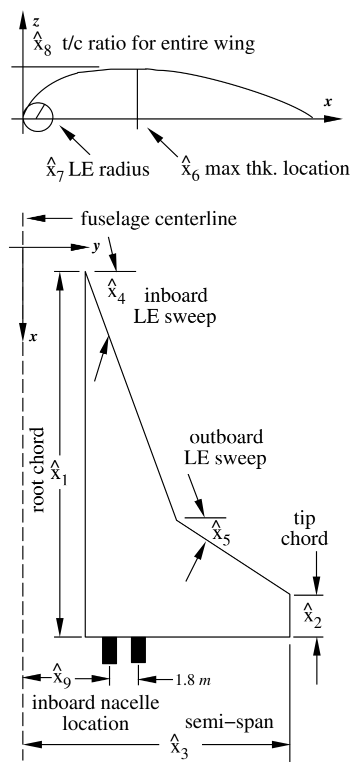

Figure 2. Variables describing the wing cross-section (top), along with the wing planform and engine nacelle location for the HSCT optimization problem.

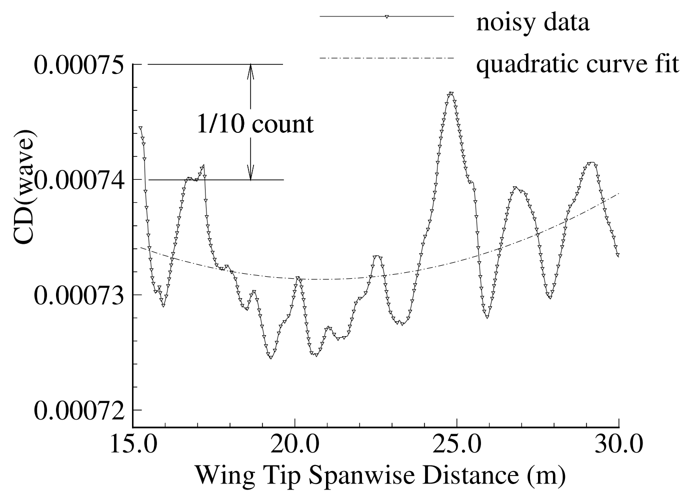

Figure 3. Numerical noise in computed wave drag.

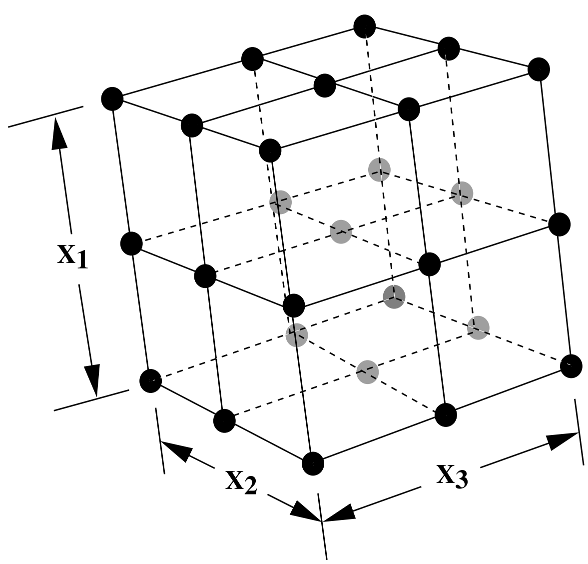

Figure 4. A 3^3 full factorial design (27 points).

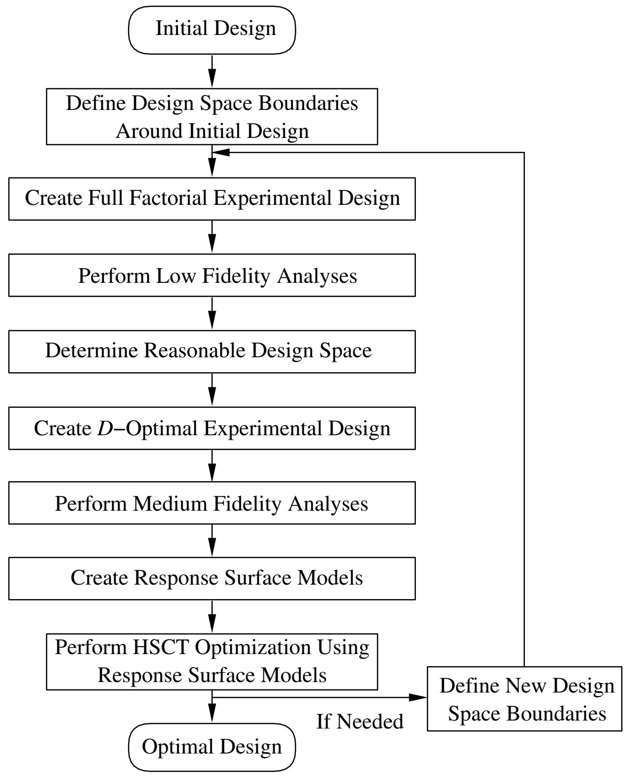

Figure 5. Flowchart depicting the use of the VCRSM method in HSCT design optimization.

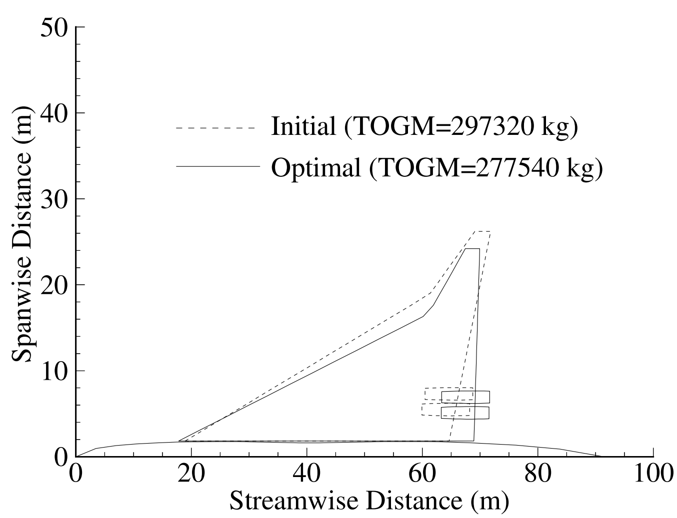

Figure 6. Ten-variable initial and optimal wing designs obtained using RS models.

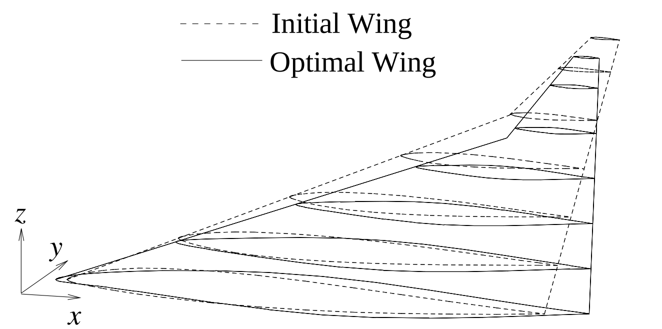

Note: The x-z plane is scaled to show airfoil differences.

Figure 7. Ten-variable initial and optimal wing designs (with RS models) showing airfoil differences.

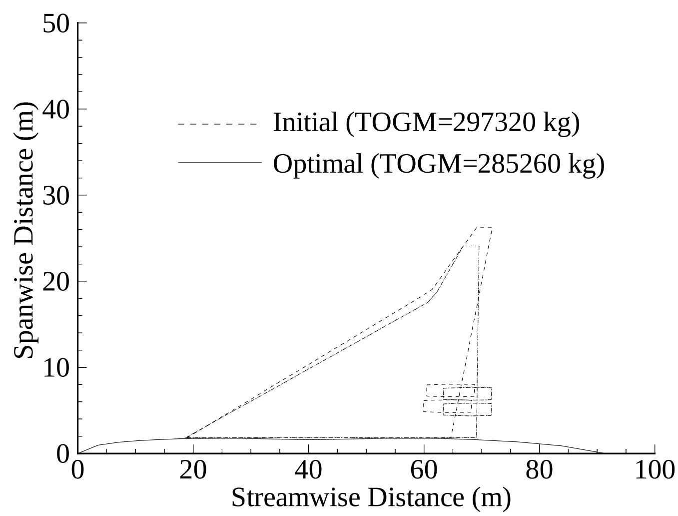

Figure 8. Ten-variable initial and optimal wing designs obtained without using RS models.